CSCanada
Energy Science and Technology
Vol. 6, No. 1, 2013, pp. 52-60
DOI:10.3968/j.est.1923847920130601.2613

ISSN 1923-8460[PRINT]
ISSN 1923-8479[ONLINE]
www.cscanada.net
www.cscanada.org

Numerical Simulation of the Multi-Level Air-Gun Array Based on Over/Under Source

LI Zhe[a],*; WANG Haikun[b]

[a]College of Information and Control Engineering, China University of Petroleum (East China), Qingdao, China.
[b]China Oilfield Services Limited, Tianjin, China.
*Corresponding auhtor.

Received 15 April 2013; accepted 3 Augutst 2013

Abstract
The conventional air-gun array is made of all guns at the same depth. This array is arranged in a simple way. It is easy to operate. But the ghost effect is obvious. And the ghost will limit the effective seismic bandwidth. Using the over/under source, we can attenuate the ghosts generated at the source side. Based on the over/under source, this paper proposes the multi-level source which consists sub-arrays placing at different depths and firing them in a sequence. This makes the notch frequencies of the sub-arrays different. After superposition, it can attenuate the source ghost. The sub-arrays in different depths are regarded as the over/under sources. Then we separate the up-going and down-going events. Data test proved that the algorithm can indeed attenuate the ghost included in the far-field wavelet, which extends the effective bandwidth and benefits low and high frequencies.

Key words: Air-gun array; Over/under source; Multi-level source; Source ghost; Numerical simulation

LI Zhe, WANG Haikun (2013). Numerical Simulation of the Multi-Level Air-Gun Array Based on Over/Under Source. *Energy Science and Technology*, *6*(1), 52-60. Available from: URL: http://www.cscanada.net/index.php/est/article/view/10.3968/j.est.1923847920130601.2613
DOI: http://dx.doi.org/10.3968/j.est.1923847920130601.2613

INTRODUCTION
The air-gun array is widely used nowadays as a source in towed streamer seismic survey. The array pattern can be used to attenuate the ghost caused by a source. Based on the single air-gun theory model of seismic exploration, a numerical simulation of the wavelet was conducted for the single air-gun and the air-gun array.

Keller and Kolodner (1956), in a paper formed "Damping of Underwater Explosion Bubble Oscillations" on the basis of much work on air-gun bubbles. Geophysicists (e.g., Ziolkowski, 1970; Schulze-Gattermann, 1972; Safar, 1976; Johnson, 1994) presented the wavelet simulation algorithms of a single air-gun, making the simulation of a real wavelet indoor possible. Safar (1976) derived an efficient design of air-gun arrays. Laws and Hatton et al. (1990) gave a method for calculating the output pressure waveform from a cluster air-gun. Parkes and Ziolkwski (1982) discussed the simulation method of the far-field wavelet of an air-gun array. The sea-surface reflection generates interferences between up- and down-going waves that ultimately limit the bandwidth of marine seismic data. This phenomenon is known as ghost. The ghost contained in the far field wavelet is affected by the depth of the air-gun. To solve this problem, Moldoveanu (2000) pointed out that the over/under source technique can be used to remove the source ghost. Hopperstad, Laws, and Kragh (2008) presented the multi-level array and the time-lapse explosion of the air-gun array excitation technique. Cambois, Long, and Parkes (2007) further studied the impact of a multi-level array of acquisition principles and design factors.

In this paper we propose a method for ghost attenuation using over/under source of sub air-gun arrays hanged in different water depths. The method improves the characteristics of source wavelet and signal to noise ratio. The theoretical simulation and the actual data show that the multi-level of air-gun array enlarges the frequency spectrum of the source wavelet and improves energy both in low frequency and high frequency.

1. THEORIES

1.1 Theory of a Single Air-Gun

For the ideal case of a spherical bubble in an infinite volume of water at hydrostatic pressure P0, the bubble motion approximately obeys:

$$\frac{d^2r}{dt^2}=\frac{p}{\rho r}-\frac{3}{2r}\frac{dr}{dt}+\frac{1}{\rho v}\frac{dp}{dt} \tag{1}$$

where r is bubble radius as a function of time t, P is the acoustic pressure at the bubble wall, ρ is the density of the water, and v is the acoustic velocity of the water. Density ρ and acoustic velocity v are assumed constant in this equation. The approximate notional signature corresponding to this, referenced to unit distance, is:

$$p(t)=r\left(p+\frac{\rho u^2}{2}\right) \tag{2}$$

where $u=(dr/dt)$ is the particle velocity at the bubble wall.

This signature is the source wavelet that propagates into the far-field with a $1/R$ attenuation of amplitude. That is, the pressure field at a distance R from the origin is $r\left(p+\frac{\rho u^2}{2}\right)/R$.

The acoustic pressure P at the bubble wall is the absolute air pressure Pa inside the bubble minus the hydrostatic pressure P_0 in the water:

$$p=p_a-p_0 \tag{3}$$

The absolute air pressure in the bubble is given by:

$$p_a=p_0\left(\frac{r_0}{r}\right)^{3\gamma} \tag{4}$$

where r_0 is the equilibrium bubble radius at hydrostatic pressure, and γ is a thermodynamic parameter having a value 1.0 for isothermal, 1.4 for adiabatic, and about 1.13 based on fitting empirical air-gun data, according to Ziolkowski (1970).

These equations by a simple modified Euler method, with the substitution:

$$\frac{dp}{dt}=\frac{-3\gamma p_a}{r}\frac{dr}{dt}=\frac{-3\gamma p_a u}{r} \tag{5}$$

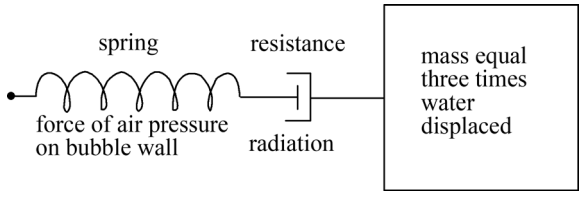

Figure 1
Harmonic Oscillator Equivalent to an Air-gun Bubble. Parameters Change with Bubble Size

1.2 Theory of Clustered Air-guns

The root cause of the bubble oscillation is the difference between the inside pressure and the outside pressure. It generates the pressure wave-field. When guns are irrelevant, the pressure outside the bubble is equivalent to the hydrostatic pressure around the bubbles, which is a constant. The external pressure of the bubble is:

$$p_d(t)=p_a(t)-p_H \tag{6}$$

where $p_a(t)$ is the pressure within the bubble, as a function of time, and p_H is the hydrostatic pressure around the bubble.

For clustered guns, the distance between the shots is small. The pressure fields generated from the bubbles will affect each other. The outside pressure is no longer a constant pressure, but equal to the sum of the hydrostatic pressure surrounding the bubbles and the pressure wave fields generated from the other bubble. Thus, the bubble external pressure should be:

$$p'_{Hi}(t)=p_H+m(t) \tag{7}$$

where $m(t)$ is the pressure wave fields generated from the other bubbles.

Substitute (7) into (6):

$$p_d(t)=p_a(t)-\left[m(t)+p_H\right] \tag{8}$$

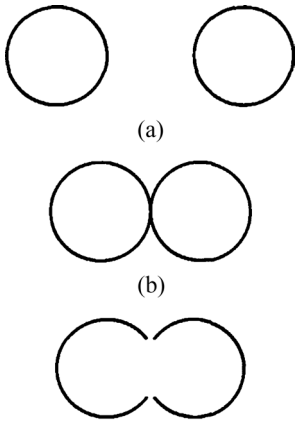

Figure 2
The Distance of the Two Guns

1.3 Theory of the Conventional Air-Gun Array

Geophysicists presented the wavelet simulation algorithms of a single air-gun, making simulate a real wavelet indoor possible.

Based on the simulation of the single air-gun, considering the propagation and the superposition of the single air-gun, we can get the far-field wavelet of the air-gun array.

A conventional air-gun array is made of several sub-arrays each containing a number of guns, or clusters of guns (Figure 3). All guns are at the same depth (typically between 5 and 10 meters) and fire at the same time. This provides constructive down-going energy but also constructive up-going energy. Therefore the ghost has the same energy as the direct wave.

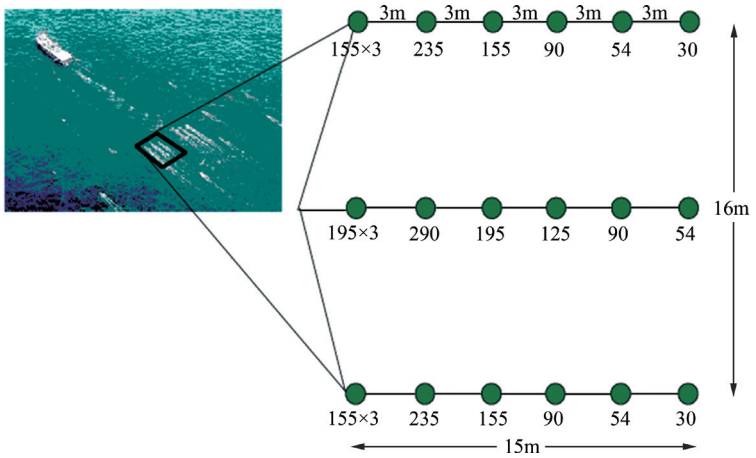

Figure 3
Plan View of Typical Air-gun Array. Numbers below the gun stations (green circles) are gun volumes (in3). The 155*3 notation indicates three guns, each with a volume of 155 in^3, so close together that their air bubbles coalesce after the guns fire. Such so-called "cluster guns" produce sound more efficiently than a single large gun (Figure courtesy of Schlumberger).

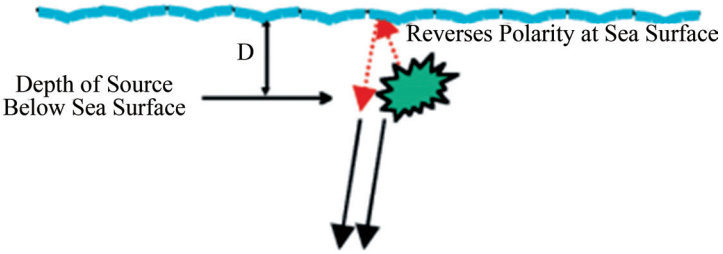

Figure 4
How a Ghost Notch is Formed

When the distances between the guns are far enough, we can consider that the interference effect between the guns does not exist. The pressure waves generated by the array can be regarded as the result of the superposition of the single guns:

$$p(t)=\sum_{i=1}^{n}\frac{1}{r_i}p_i\left(t-\frac{r_i-1}{c}\right) \tag{9}$$

where $p_i(t)$ is the wavelet from the ith gun, and r_i is the distance between the ith gun and the hydrophone; c is the speed of the sound in water.

Considering the ghost (Figure 4), Parkes and Ziolkwski (1984) presented that if there are n guns, and put a hydrophone 1 m away from each gun, then the output $h_j(t)$ of each of the hydrophones is as follows:

$$\frac{h_j(t)}{s_j}=\sum_{i=1}^{n}\frac{1}{r_j}p_i'\left(t-\frac{r_j-1}{c}\right)-\sum_{i=1}^{n}\frac{R}{(r_g)_j}p_i'\left(t-\frac{(r_g)_j-1}{c}\right)$$

where $p_i'(t)$ is the ith notional source signature, and r_{ij} is the distance between the ith gun and the jth hydrophone; c is the speed of the sound in water. The ghosts of the notional sources are accounted for by the second summation, in which the distance $(r_g)ij$ is between the virtual image of the ith gun and the jth hydrophone. R is the reflection coefficient at the sea surface (normally is -1) and s_j is the sensitivity of the jth hydrophone.

Using the inverse Fourier transform of X, we can obtain the notional source pressure signatures in time-domain. Then the signature of the far-field at any point can be calculated:

$$f(w)=\sum_{i=1}^{n}p_i(w)\left[\frac{1}{r_i}\exp\left(iw\frac{r_i-1}{c}\right)-\frac{1}{(r_g)_i}\exp\left(iw\frac{(r_g)_i-1}{c}\right)\right]$$

Where $p_i'(w)$ is the ith source pressure signature in frequency-domain, and $f(w)$ is the far-field signature calculated in frequency-domain.

The equation (11) is equivalent to:

$f(w)=A'X$

Where X means the source pressure signatures in frequency-domain,

$$A'=\left[\frac{1}{r_1}\exp\left(iw\frac{r_1-1}{c}\right)-\frac{1}{(r_g)_1}\exp\left(iw\frac{(r_g)_1-1}{c}\right),\cdots,\right.$$
$$\left.\frac{1}{r_n}\exp\left(iw\frac{r_n-1}{c}\right)-\frac{1}{(r_g)_n}\exp\left(iw\frac{(r_g)_n-1}{c}\right)\right]$$

The inverse Fourier transform of $f(w)$ is the far-field signature in time-domain.

1.4 Theory of the over/Under Source

In marine towed-streamer acquisition, seismic resolution is limited by source and receiver ghosts. Figure 5 shows the amplitude spectra of seismic data recorded with sources deployed at 8 m and 30 m. The source deployed at 30 m reserves the low frequencies but the ghost notch repeats every 25 Hz and destroys the higher frequencies. The shallow source better preserves the higher frequencies but the notch at zero Hz attenuates the lower frequencies. The key geophysical issue that must be resolved in order to improve the seismic bandwidth of towed-streamer data is to remove the ghost notches, a process known as de-ghosting.

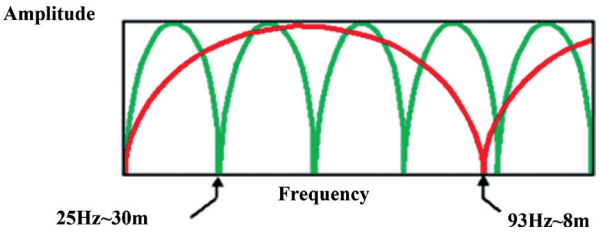

Figure 5
Amplitude Spectrum for Sources Deployed at 8m (Red) and 30 m (Green)

Separation of the up-going seismic wave-field from the down-going seismic wave-field, which contains the ghost reflections, is a well-known de-ghosting method. The wave-field separation method described in this section is based on a technique proposed by Bell and Cox (1987) for VSP processing.

Assume a hypothetical source *S* placed at the midpoint between the two sources (Figure 6). This source *S* generates up-going and down-going source wave-fields at a reference time *t*.

$$S=u(t)+d(t) \tag{12}$$

Based on the method of Bell and Cox the down-going wave-field $d(t)$, can be obtained as:

$$d(t)=\left(S_1+S_2-I/T\right)/4 \tag{13}$$

where *Sum* is the sum of S_1 and S_2, I is the integral of the difference of S_1 and S_2, and T is the half the travel time between the two source levels.

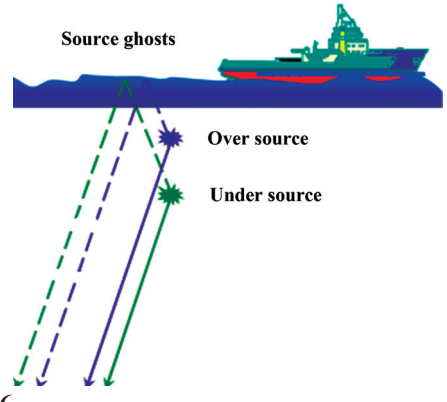

Figure 6
The Principle of Over/Under Combination

The over/under sources were implemented with two source arrays placed in the same vertical plane and at two different depths (Figure 7). The depth of the first array was 6 m and the depth of the second array was 11 m. The inline separation of the two arrays was 37.5 m which was equal with the shot-point interval. The sources were fired in flip-flop mode, such that two shots were generated at the same *x, y* location, but, at different depths. This manufactured the desired over/under source geometry.

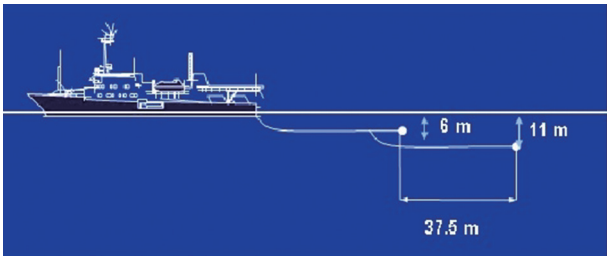

Figure 7
Implementation of Over/Under Sources

1.5 Theory of the Multi-level Air-gun Array

The multi-level source concept puts guns, clusters or sub-arrays at different depths and fires them sequentially so that only the down-going waves builds up constructively. The up-going wave does not build constructively and the ghost effects are consequently reduced. Figure 9 shows the ghost signatures for the two schematic sources represented in Figure 8 (assuming a nominal depth of 7.5m). The multi-level source displays a longer and lower-amplitude ghost arrival. Its amplitude spectrum is flatter than for a conventional source: more extended towards the high and low frequencies but trimmed in the mid-frequency range. This is what we should expect from de-ghosting: on the one hand we fill the notches created by the ghost, but on the other hand we no longer benefit from the boosting effect at other frequencies.

An important issue to consider with the multi-level source is the radiation pattern. The geometry used in Figure 8 clearly shows that a direction other than down-going also benefits from the beam steering. That constructive energy in the upper-right corner of the last panel could be eliminated by changing the gun pattern: switching the depth and firing time of the two first guns for example. However, this would simply displace the problem as another direction will be favored by the new beam steering geometry. Although conventional source arrays also have a radiation pattern and are far from being isotropic, this issue is more pronounced with the multi-level source. Array modeling is required to ensure the spectral benefits are not offset by unintended consequences.

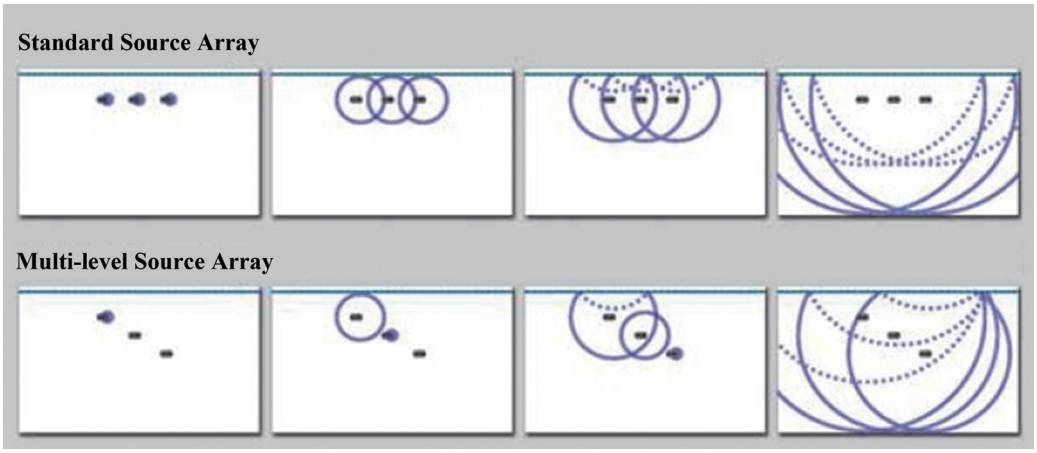

Figure 8
A Conventional Source Array (Upper) Fires All Guns Simultaneously Generating Constructive Down-going Wave (Solid) and Ghost (Dashed). The sequential firing of the multi-level source (lower) builds a constructive down-going wave but not a constructive ghost. Note however the constructive energy on the upper-right corner of the last panel.

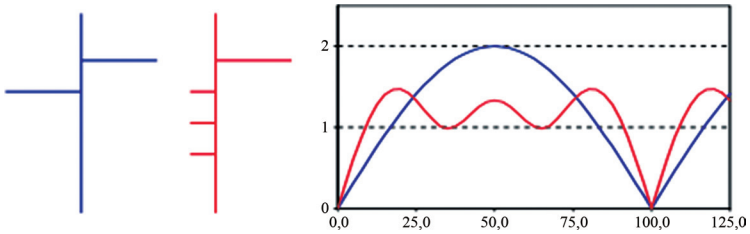

Figure 9
Ghost Signatures for the Standard (Blue) and Multi-level (Red) Sources of Figure 8. The multi-level ghost has three lower-amplitude arrivals. Its corresponding spectrum shows more energy in the high and low frequencies, but less in the mid-frequency range.

Beyond the change in ghost behavior, the air-gun signature is also affected by the new design. First, the source ghost is an effective attenuator of bubble pulses. Consequently, we expect the multi-level source to deliver a lower peak-to-bubble ratio (PTB) than a conventional source. Second, since the guns are towed deeper they operate under higher hydrostatic pressure, which reduces the size of their bubble. Smaller bubbles mean less low frequency content, which can partly offset the gains shown in Figure 9. Third, the reduced diversity in bubble sizes means less flexibility in array design and bubble pulse attenuation. Therefore, modeling is the key to ensuring an effective multi-level source array design.

2. RESULTS: SINGLE GUN TEST

2.1 Result: Single Gun Test

Based on theoretical model of a single gun, we simulate the far-filed wavelet of a sleeve gun .Then we compare it with the actual measured far-field wavelet. The working pressure of the air-gun is 2000psi.The volume of the air-gun is 150in3.The depth of the air-gun is 6m.And the acoustic velocity of the water is 1500 m /s. In Figure 3 we show the wavelets computed using the method compared with the wavelet measured. The comparative of quality parameters of the wavelets is given in Table 1.

Table 1
Parameters of the Measured Wavelet and the Calculated Wavelet

	A (bar.m)	T (ms)	P / B
Measured	3.35	88.2	2.92
Calculated	3.39	95	2.93

Figure 10 and Table 1 show, both the waveform and the quality parameters of the two wavelets are very consistent, which indicate the correctness and feasibility of the simulation.

2.2 Result: Conventional Array Test

To test the accuracy and the stability of the method, the sub-array shown in Figure 11 is used.

The depth of the array is 6 m. The reflection coefficient at the sea surface is -1. The sampling interval is 1.0 ms, and the speed of sound in water is 1521.6 m/s. The density of the water is 1030kg/m^3.The working pressure of the air-guns is 2000 psi (1psi=6.894757kPa). The position of the air-guns and the volume parameters are in Table 2.

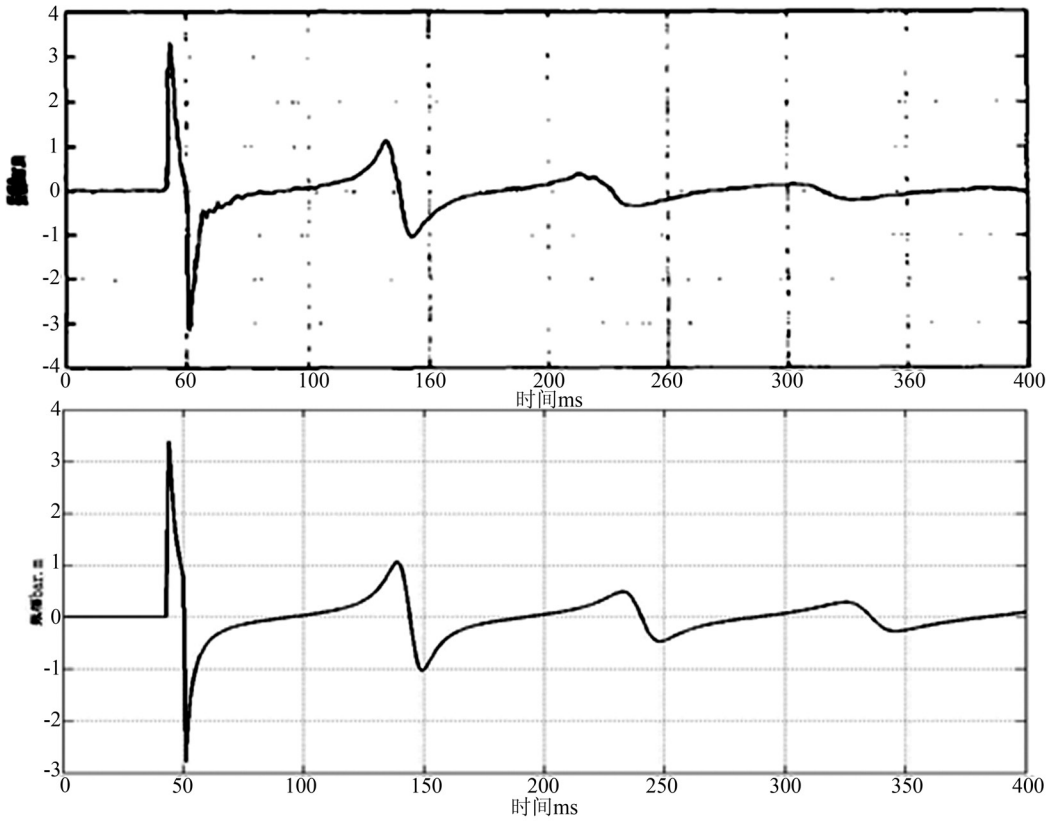

Figure 10
Comparison of the Measured Wavelet (Upper) and the Calculated Wavelet (Lower)

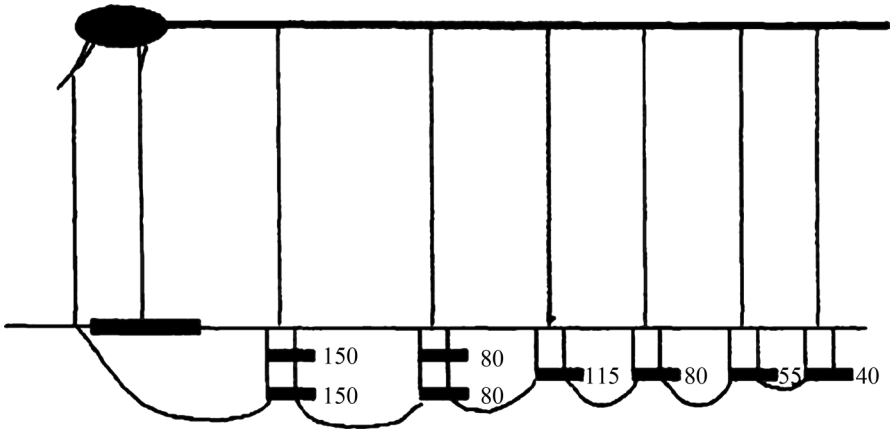

Figure 11
The Positions of the Guns

Table 2
Parameters of the Sub-Array

GUN#	X(m)	Y(m)	Z(m)	V(in^3)
1	0	0	5.5	150
2	0	0	6.5	150
3	4.3	0	5.5	80
4	4.3	0	6.5	80
5	7.6	0	6	115
6	10.4	0	6	80
7	12.9	0	6	55
8	15.1	0	6	40

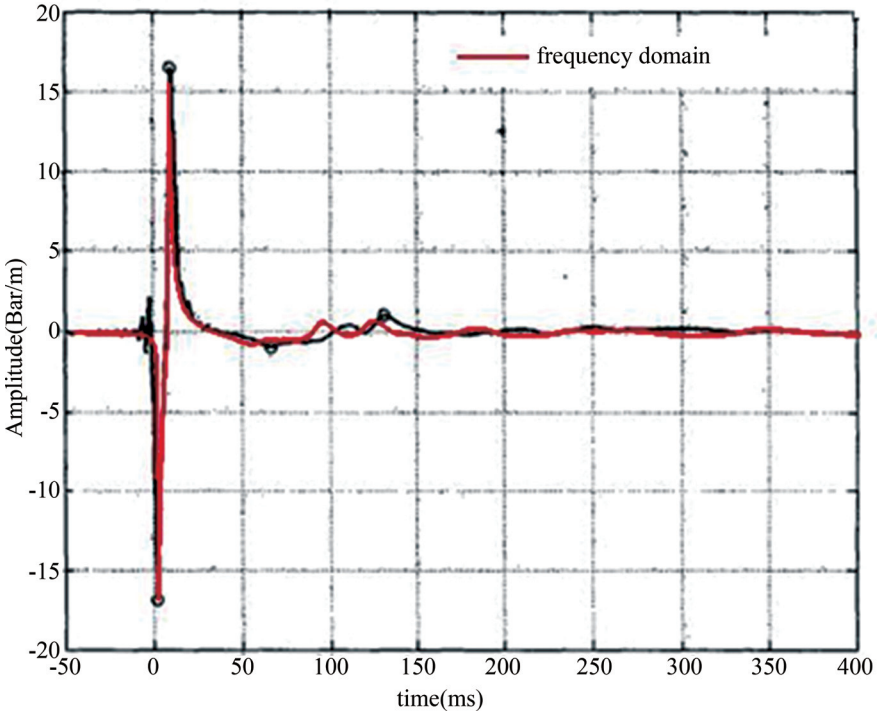

Figure 12
Comparison of the Measured Wavelet (Black Line) and the Calculated Wavelet (Red Line)

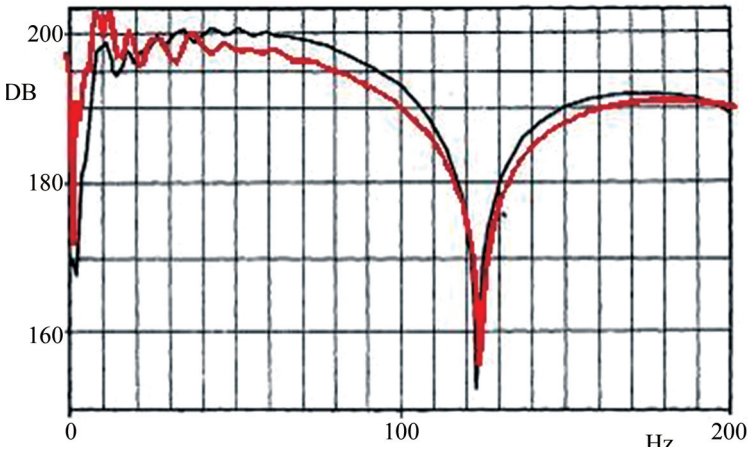

Figure 13
Comparison of the Spectrum of the Measured Wavelet (Black Line) and the Calculated Wavelet (Red Line)

The comparative of the far-field wavelet simulated and the actual measurement obtained from the air-gun array is shown in Figure 12. It can be seen that waveforms and the peak values of the two wavelets are very consistent. While Figure 13 shows the spectrums are also in good agreement. This shows that the simulation algorithm of the air-gun array is practicable.

2.3 Result: Multi-level Array Test

To illustrate the superiority of the multi-level array, we use three groups of the sub-array shown in Figure 11.

The depth of the second sub-array is 6 m when the array is a planar array. And the depth of the second sub-array is 7 m when the array is a multi-level array.

As can be seen from the wavelets (Figure 14) of the two models, the multi-level array generates a smoother far field wavelet, better suppression of the bubble pulse. The PTB of the plane model is 25.14%, while the PTB of the multi-level model is 33.11%. The multi-level array has more advantages. Meanwhile, the comparative of the spectrums shown in Figure 15 also shows the spectrum of the wavelet generated form the multi-level array has a wider effective band, stronger energy of the high and low frequency. And the notch point of the multi-level array is higher than that of the conventional planar array, which indicates that multi-level array indeed has suppression notch.

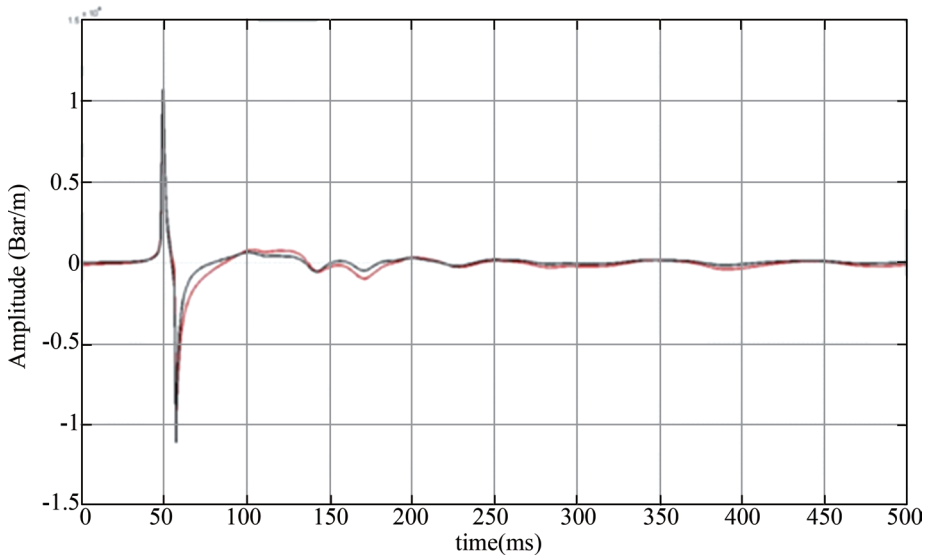

Figure 14
Comparison of the Conventional Array (Red Line) and the Multi-level Array (Black Line)

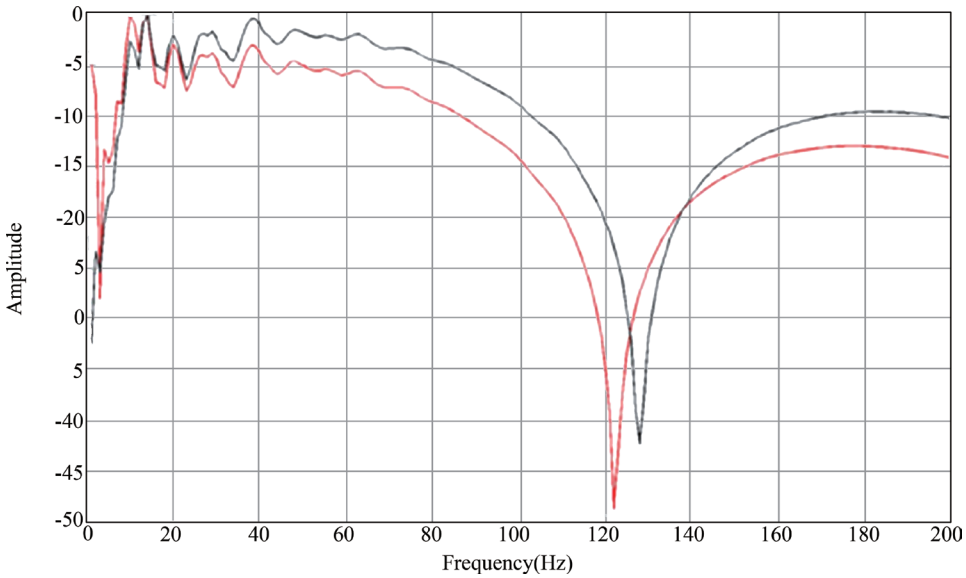

Figure 15
Comparison of the Spectrum of the Conventional Array

CONCLUSIONS

In this paper, on the basis of the simulation of the wavelet from the single air-gun and air-gun array, we use a combination of over/ under source to solve the problem of the ghost of marine seismic exploration. Through the test of single air-gun and the air-gun array, we could obtain the conclusions as follows:

- Compared with the plane array, the multi-level array can more efficiently suppress the notch caused by ghost reflection at sea level, and has more smooth frequency spectra.
- In addition,the multi-level array is important to further detailed researches and tests due to its effect to improve wavelet quality.

ACKNOWLEDGMENTS

The authors would like to thank the China Oilfield Services Limited for their cooperation in providing the data and support.

REFERENCES

Bell, D. W., & Cox, V. D. (1987). Two-trace directional filter for processing offset VSPs. *57th Annual International Meeting, SEG, Expanded Abstracts*, 768-769.

Cambois, G., Long, A., Parkes, G., Lundsten, T., Mattsson, A., & Fromyr, E. (2009, June). Multi-level air gun array—a simple and effective way to enhance low frequencies in marine seismic. Paper presented at the 71st AGE Conference and Exhibition, Amsterdam, The Netherlands.

Egan, M., El-Kasseh, K. G., & Moldoveanu, N. (2007). Full deghosting of OBC data with over/under source acquisition. *SEG Technical Program Expanded Abstracts*, 31-34.

Hopperstad, J., Laws, R., & Kragh, E. (2008, June). Fundamental principles of isotropic marine source design. Paper presented at the 70th EAGE Conference and Exhibition, Rome, Italy.

Keller, J. B., & Kolodner, I. I. (1956). Damping of underwater explosion bubble oscillations. *Journal of Applied Physics*, *27*(10), 1156-1161.

Laws, R. M., Hatton, L., & Haartsen, M. (1990). Computer modeling of clustered air guns. *First Break*, *8*(9), 331-338.

Moldoveanu, N. (2000). Vertical source array in marine seismic exploration. *70th Annual International Meeting, SEG, Expanded Abstracts*, 53-56.

Parkes, G. E., Ziolkowski, A., & Hatton, L. et al. (1984). The signature of an air gun array, Computation from near-field measurements including interactions-Practical considerations. *Geophysics*, *48*(2), 105-111.

Safar, M. H. (1976). Efficient design of air-gun arrays. *Geophysical Prospecting*, *24*, 773-787.

Ziolkowski A., Parkes, G., & Hatton L., et al. (1982). The signature of an air gun array, Computation from near-field measurements including interactions. *Geophysics*, *47*(10), 1413-1421.

Ziolkowski, A. (1970). A method for calculating the output pressure waveform from an air gun. *Geophysics*, *21*, 137-161.

